Carbon 129 (2018) 428–437

Contents lists available at ScienceDirect

Carbon

journal homepage: www.elsevier.com/locate/carbon

Graphene oxide affects *in vitro* fertilization outcome by interacting with sperm membrane in an animal model

Nicola Bernabò [a, *, 1], Antonella Fontana [b, 1], Marina Ramal Sanchez [a], Luca Valbonetti [a], Giulia Capacchietti [a], Romina Zappacosta [b], Luana Greco [a], Marco Marchisio [c, d], Paola Lanuti [c, d], Eva Ercolino [c, d], Barbara Barboni [a]

[a] Faculty of Bioscience and Technology for Food, Agriculture and Environment, University of Teramo, 64100 Teramo, Italy
[b] Department of Pharmacy, University "G. d'Annunzio" Chieti-Pescara, 66100, Chieti, Italy
[c] Department of Medicine and Aging Sciences, University "G. d'Annunzio" Chieti-Pescara, 66100, Chieti, Italy
[d] Center on Aging Sciences and Translational Medicine (CeSI-MeT), University "G. d'Annunzio" Chieti-Pescara, 66100 Chieti, Italy

ARTICLE INFO

Article history:

Keywords:
Spermatozoa
Graphene oxide
In vitro fertilization
Membranes
Cholesterol

ABSTRACT

We realized the exposure of boar spermatozoa to graphene oxide (GO) at concentration of 0.5, 1, 5, 10 and 50 μg/mL in an *in vitro* system able to promote the capacitation, i.e. the process that allows sperm cells to became fertile. Interestingly, we found that the highest GO concentration (5, 10 and 50 μg/mL) are toxic for spermatozoa, while the lowest ones (0.5 and 1 μg/mL) seem to significantly increase the sperm cells fertilizing ability ($p > .05$) in an *in vitro* fertilization experiment. To explain this finding, we investigated the effect of GO on sperm membrane structure (atomic force microscopy) and function (confocal microscopy and flow cytometry, substrate adhesion). As a result, we found that GO is able to interact with spermatozoa membranes and, in particular, it seems to be able to extract the cholesterol, which is a key player in spermatozoa physiology, from plasma membrane of boar spermatozoa incubated under capacitation conditions. In our opinion, these results are very important because they allow identifying either a plausible mechanism of GO toxicity on spermatozoa and new strategies to manage sperm capacitation.

1. Introduction

Graphene has recently received special attention in the research world due to its exceptional properties ranging from materials science to physics, electronics, optics and mechanics [1–4]. Graphene is a one atom thick molecule formed mainly of sp^2 hybridized carbon atoms. For this reason it is considered a two-dimensional material characterized by an exceptional strength, a high aspect ratio, an extraordinary thermal and electrical conductivity and a substantial transparency [2]. In the last five years a lot of studies have been performed on the capacity of some hydrophilic derivatives such as graphene oxide or reduced graphene oxide to favour stem cells differentiation [5–7], to induce synaptic connections in healthy primary neurons [8] as well as to strengthen or confer elasticity to biomaterials [9,10]. Preferential use of hydrophilic derivatives rather than pristine graphene in these studies is due to the fact that pristine graphene, despite its exceptional features, is difficult to disperse and process. Graphene oxide (GO) is instead promptly dispersible in water and, although it presents oxygen functionalities that affect the integrity of the honeycomb lattice of pristine graphene, keeps the majority of its properties.

The growing use of GO as biomaterial in recent years bring to light many important questions regarding its possible toxicity to organs, tissues and cells. In literature there are several papers addressing this issue, with specific regards to erythrocytes and fibroblasts [11], pheochromocytoma-derived PC12 [12], A549 [13], and human mesenchymal stem cells (hMSCs) [13,14]. In this context, one of the most interesting field of study would be the characterization of the GO exposure effect on reproductive function. This could have very important implications because of the key function of reproduction for all the organisms and because alteration on gametes could affect successive generations. Ultimately, the reproduction is the result of the interaction of gametes

* Corresponding author.
E-mail address: nbernabo@unite.it (N. Bernabò).
[1] Equally first authors.

https://doi.org/10.1016/j.carbon.2017.12.042

(the oocyte and the spermatozoa) within the female genital tract, where the spermatozoa complete the process that allows them to reach the ability to fertilize (the capacitation). Capacitation process takes from several hours to days, in which spermatozoa are exposed to a myriad of environmental factors and, eventually, exogeneous molecules able to modulate their physiological and biochemical machinery.

Indeed, a key point for biomedical applications of graphene derivatives and GO is their capacity to interact with biomolecules either via covalent and non-covalent interactions. In the former case covalent functionalization is mainly obtained by exploiting the ability of the enriched oxygen functional groups of GO to immobilize the biomolecules through nucleophilic substitutions or other similar reactions [15]. On the other hand, non covalent interactions such as $\pi-\pi$, van der Waals or electrostatic interactions may significantly affect the fate of these materials in biological systems including their cellular uptake and consequent biocompatibility [5]. Data are rather conflicting essentially due to the fact that all biological responses of GO vary depending on the number of layers of the investigated graphene, lateral size, hydrophobicity, surface functionalization, colloidal stability and concentration [16]. In particular, Yue et al. have investigated [17] the viability and cell responses of six different cell lines upon addition of GO of different dimensions. They discovered that only two phagocitic cell lines were able to internalize both nano- and micro-sized GO sheets and that almost no difference in terms of viability was detected in the six cells lines for concentration of GO lower than 20 μg/mL. In another study, the investigation of the interactions between GO and plasma membrane and the subsequent uptake of GO by macrophages, allowed to evidence [18] that large microsized GO sheets were prevailingly detected parallel and adsorbed to plasma membranes, while a high amount of smaller GO sheets were taken up by the cells after 6 h of incubation. From these examples, the interactions of GO with cell membrane appear to be crucial for investigating the toxicity and the effects of GO on cells. For this reason, and aware that virtually all the signalling systems involved in driving the communication of spermatozoa with female environment are located at membrane level, because male gametes are transcriptionally silent and their lipid metabolism is very limited [19,20], we thought it is noteworthy to investigate GO-spermatozoa interactions.

In this context the presence of GO could promote biologically relevant effects on male gametes, thus affecting the fertilization process. For this reason we studied the effect of GO on spermatozoa functional parameters during capacitation. In our work, we used an *in vitro* animal model because of the possibility to control all the environmental parameters and to work in the absence of ethical issues concerning manipulating animal gametes and embryos.

2. Results

2.1. GO characterization

In order to ascertain that the investigated GO could not be internalized in the cells we used micrometer sized GO, that demonstrated to interact prevailingly with the plasma cells without entering them [18]. In particular, intensity DLS data (Table 1) indicate a mean diameter of 800 ± 30 nm for the 0.5 μg/mL GO dispersions at 38.5 °C and the size do not increase on increasing the GO concentration, thus confirming the producer micrometer sized GO and its scarce tendency to aggregate at these concentrations. Polydispersity data evidence, as expected, the presence of a moderately polydispersed sample, ranging from 0.202 to 0.345. The irregular shape of GO flakes (see Fig. 1) contributes to the polydispersity of the sample. DLS measurements could not be performed in TMC199 due to the presence in the pure TMC199 of aggregates of micrometric dimensions (>5000 nm, data not shown). The obtained zeta potential changes between -26 ± 1 at 0.5 μg/mL GO and -54 ± 1 mV at 50 μg/mL in distilled water thus indicating a stable dispersion in which electrostatic repulsions keep GO flakes well dispersed. The presence of prevailingly single-layered or double-layered sheets of GO was verified by AFM measurements as evidenced by the high profile of Fig. 1. AFM images confirm the absence of obvious agglomeration in the sample.

2.2. GO cytotoxicity and acrosome damage

Since we used for the first time GO in a protein free system, firstly we assessed the concentration of GO able to promote a toxic effect on cell viability and on acrosome integrity. As it is shown in Fig. 2, the GO concentrations exceeding 5 μg/mL are directly toxic for spermatozoa, reducing their viability starting from the first hour of incubation. The effect on acrosome integrity starts to become statistically relevant ($p < .05$ vs. CTRL) at 5 μg/mL, while at lower concentration it appears to be negligible ($p > .05$ vs. CTRL).

2.3. Effect of GO on in vitro fertilizing ability of spermatozoa

For the first time, here, we assessed the effect of GO on fertilizing ability of spermatozoa on an animal model. As depicted in Table 2 it is evident a dose dependent-effect of GO.

In particular we have found the percentage of fertilized oocytes changed significantly ($p < .05$ vs. CTRL) at the different GO concentrations.

2.4. Functional characterization of GO interaction with sperm membranes

Under control conditions, sperm membranes become progressively more fluid (fusogenic) and as assessed by FRAP (see Fig. 3), the diffusion coefficient of DilC12 significantly increases (2.641 [1.330–5.260] vs. 6.505 [2.171–11.185] calculated diffusion coefficient (CDC) $cm^2/sec \times 10^9$, $p < .001$) (see Fig. 4 panel 1).

The presence of GO, at different concentrations, affected as well fluidity with values of 1.519 [1.023–3.444] at 0.5 μg/mL; 0.993 [0.015–4.5978] at 1 μg/mL and 4.556 [1.513–8.510] at 5 μg/mL $p < .001$) (see Fig. 4, panel 1). For the results of statistical analyses refer to Table 3.

Since the process of lipid remodelling that promotes the capacitation-dependent increase in membrane fluidity affects differently the functionally different sperm subpopulation present in the experimental system, we represented the GO-induced changes in CDC in Fig. 4, panels 2–6.

Interestingly, the treatment with GO could negatively interfere with the capacitation-dependent increase in membrane fluidity.

Since in the lipid remodelling and in the increasing of

Table 1
Size and zeta-potential of GO in water at 38.5 °C obtained by DLS.

Size (nm) [Polydispersity]	GO 0.5 μg/mL	GO 1 μg/mL	GO 5 μg/mL	GO 10 μg/mL	GO 50 μg/mL
Size (nm) [Polydispersity]	800 ± 30 [0.236]	670 ± 50 [0.318]	440 ± 35 [0.345]	540 ± 10 [0.249]	510 ± 50 [0.272]
Zeta-potential	-26 ± 1	-42 ± 2	-51 ± 1	-52 ± 1	-54 ± 3

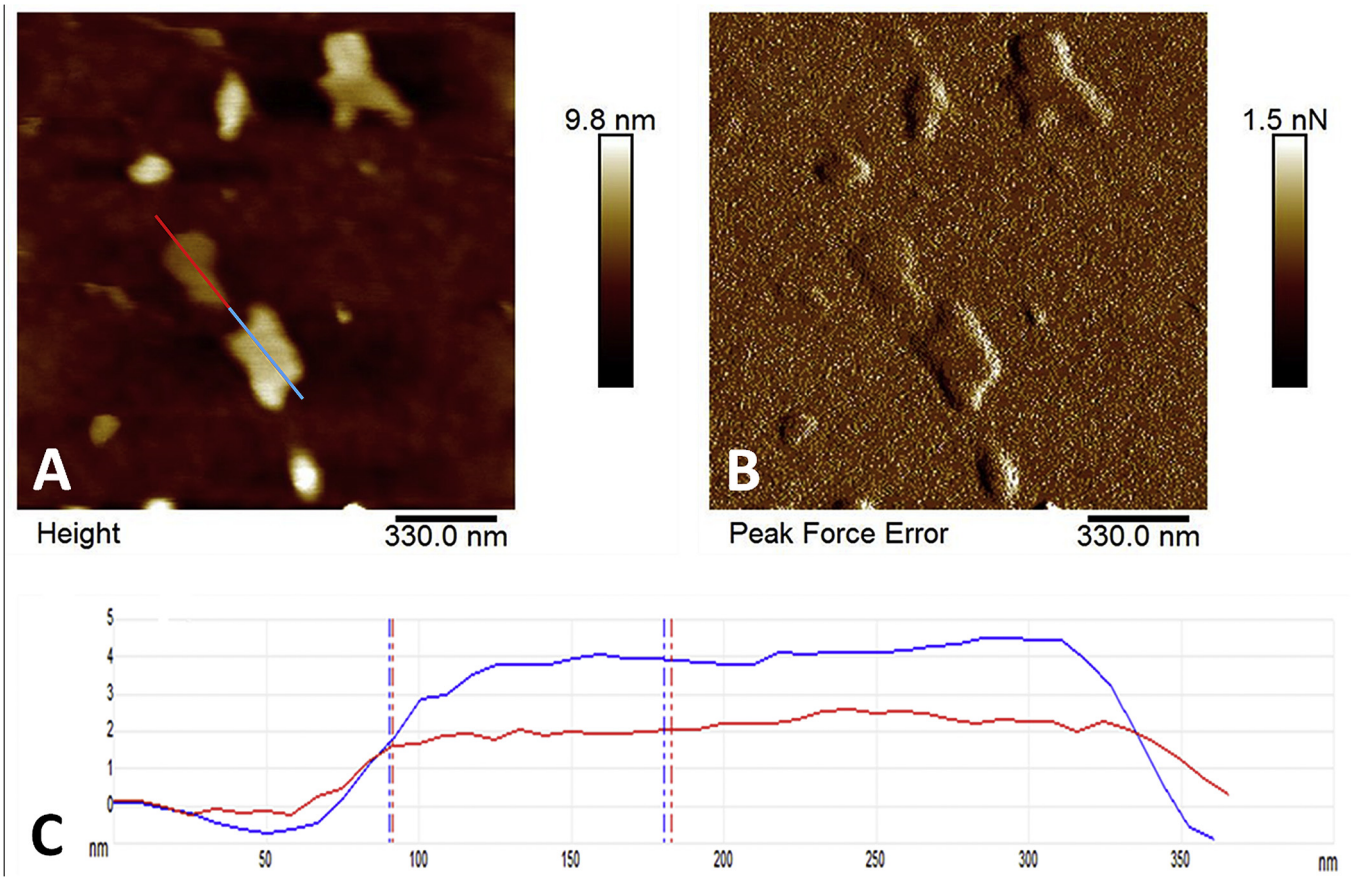

Fig. 1. AFM image, obtained operating in Peak Force QNM mode with ScanAsyst Air®, of a 0.5 μg/mL dispersion deposited by spin coating onto a SiO_2 wafer (upper images) reporting (A) topography (1.5 μm × 1.5 μm), (B) peak force error and (C) cross-section along the cross line (evidenced in image A). Scale bar is: 330 nm. (A colour version of this figure can be viewed online.)

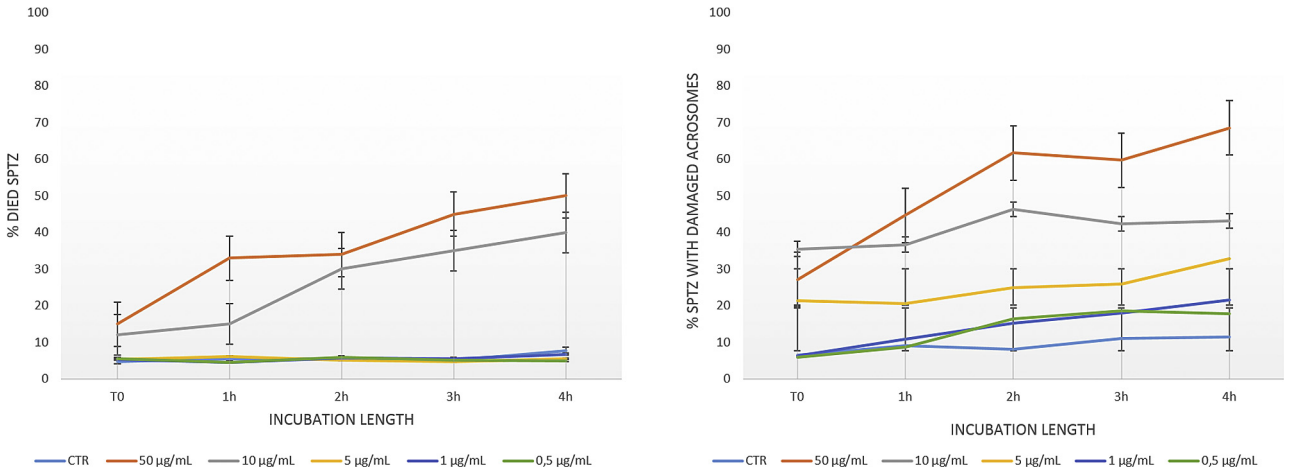

Fig. 2. Percentage of died (left graph) or spermatozoa with damaged acrosomes (right graph) at different concentration of added GO and at different times of incubation under capacitating conditions. The data are expressed as mean ± standard deviation and were analysed with ANOVA two ways. Different superscripts indicate statistically different datasets. (A colour version of this figure can be viewed online.)

Table 2
Effect of different GO concentration on IVF outcome.

	CTRL	GO 0.5 μg/mL	GO 1 μg/mL	GO 5 μg/mL
Fertilized oocytes (%)	56.6 ± 4.5^{a}	72.2 ± 3.7^{b}	87.9 ± 13.7^{c}	28.3 ± 15.6^{d}
Polyspermic oocytes (% on fertilized oocytes)	64.3 ± 13.6	72.4 ± 6.8	60.1 ± 5.3	75.9 ± 22.1
N° of spermatozoa per polyspermic oocyte	4.1 ± 0.0	3.5 ± 0.4	3.5 ± 0.5	3.3 ± 0.3

Different superscript denote statistically different groups of data ($p < .05$).

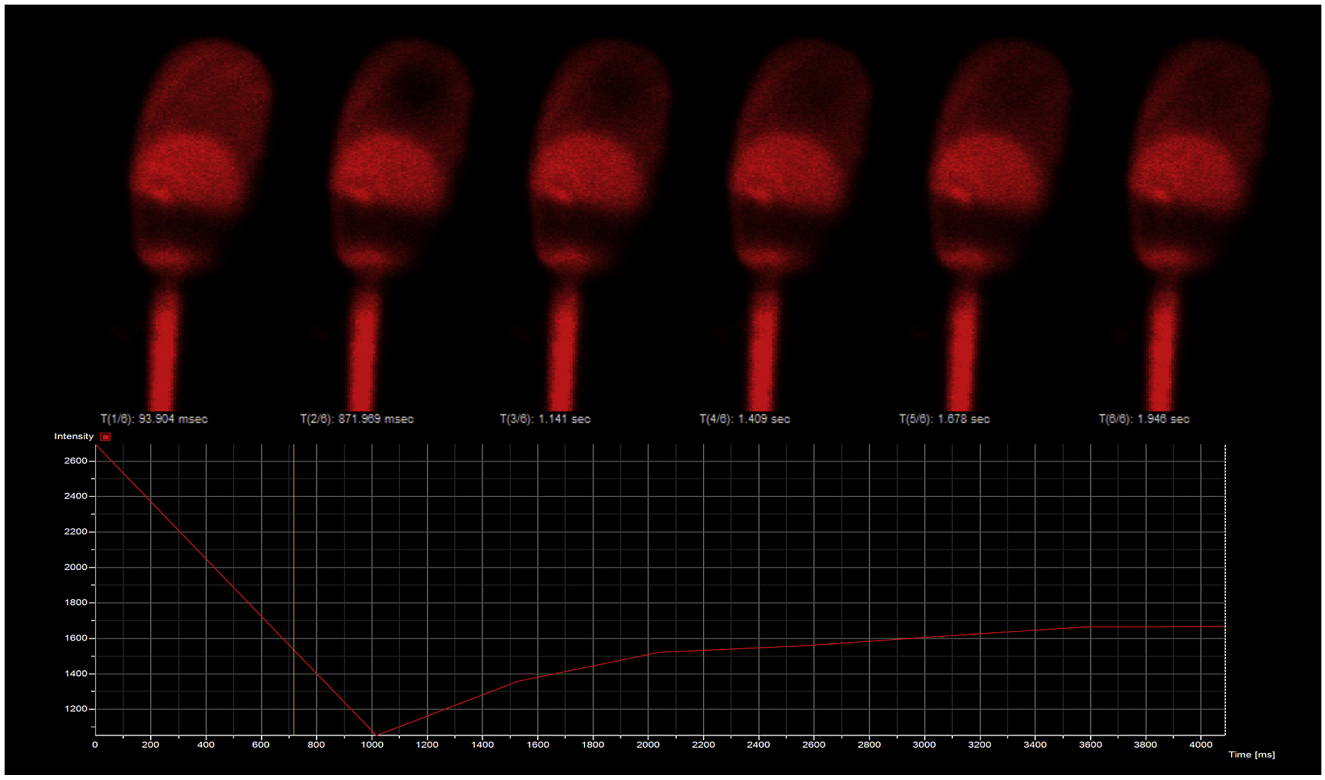

Fig. 3. Upper panel: gallery of confocal microscopy images of a spermatozoon stained with DilC12 during a Fluorescence recovery after photobleaching (FRAP) experiment. Lower panel: graph showing the analysis of data obtained in FRAP experiment. (A colour version of this figure can be viewed online.)

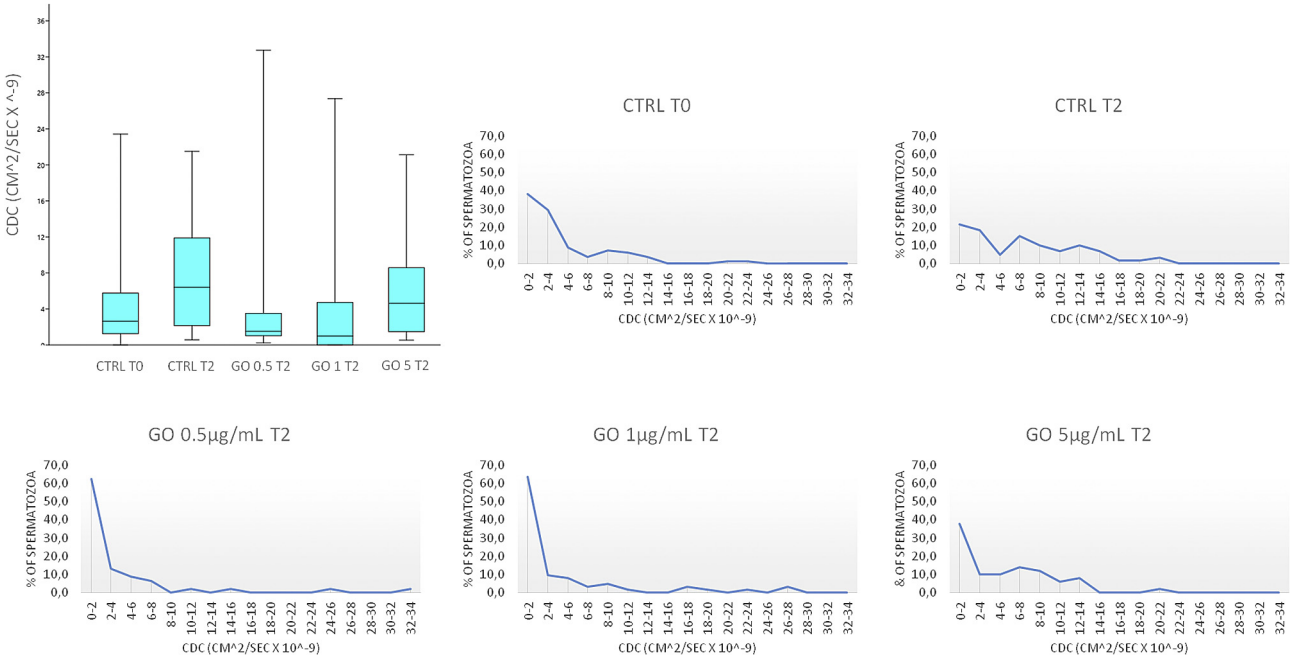

Fig. 4. Graphs showing the effect of boar spermatozoa incubation at different times in control (CTRL) conditions or in the presence of different concentration of GO on membrane fluidity, as calculated diffusion coefficient (CDC) of DilC12 in FRAP experiments. The first graph (a) represents the data referred to the different compared samples, the others represent the different subpopulation in each sample. The data were represented in boxplots as median, 25° and 75° percentile and minimum and maximum values. The data referred to the statistical analysis of data reported in Table 3. (A colour version of this figure can be viewed online.)

membrane fluidity the trafficking of cholesterol plays a key role, we used confocal microscopy to identify different patterns with filipin III (a stain that complexes cholesterol). Coherently with our previous works [21], we identified two different patterns (see Fig. 5): one characterized by higher fluorescence emission, with the positivity for filipin located in the acrosomal area and in the tail and a second pattern characterized by a lower fluorescence emission by sperm head.

Table 3
Results of statistical analysis of FRAP data. The reported values represent the p value obtained by comparing the different data sets with Kruskal-Wallis test followed by Mann-Whitney pairwise post-hoc test. A total number of 300 spermatozoa were analyzed.

	CTRL	CTRL 2 h	GO 0.5 μg/mL	GO 1 μg/mL	GO 5 μg/mL
CTRL		0.001	0.053	0.001	0.092
CTRL 2 h	0.001		0.000	0.000	0.065
GO 0.5 μg/mL	0.053	0.000		0.030	0.003
GO 1 μg/mL	0.001	0.000	0.030		0.000
GO 5 μg/mL	0.092	0.065	0.003	0.000	

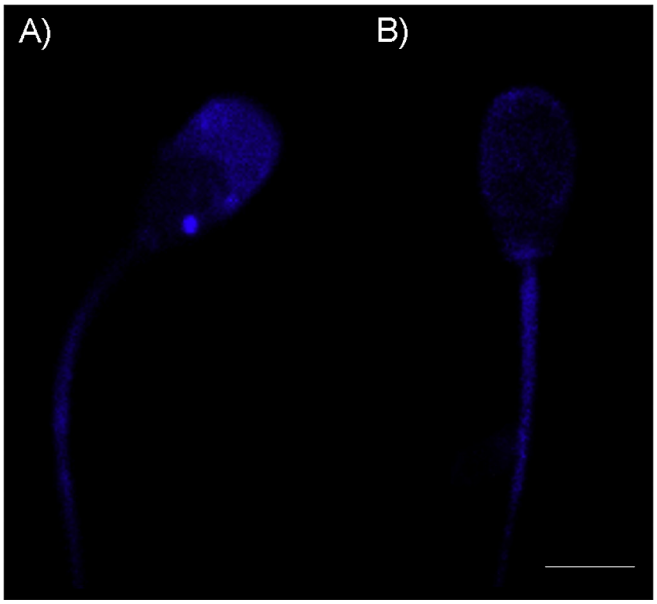

Fig. 5. Confocal micrograph of highly emitting spermatozoon (A) and low emitting spermatozoon (B) stained with filipin III. (A colour version of this figure can be viewed online.)

To characterize the evolution of the patterns occurring during the incubation under capacitating condition either in control conditions or in the presence of GO, we carried out flow cytometry experiments.

With this analytical approach, we identified five different subpopulation (P1-P5) on the basis of Side-scattered light (*SSC*), proportional to cell granularity, and filipin III emission intensity, which is related to the cholesterol content (Fig. 6). We excluded from our analysis P1 because it is constituted by cell debris and particles present in the samples, and we addressed our attention to the highly emitting population P4 and P5. P5 is characterized by very high values of SSC, thus including spermatozoa with membranes with granular structure (reacted spermatozoa or groups of adherent spermatozoa), P4 represents the subpopulation of spermatozoa with integer membranes and rich in cholesterol. It increases during capacitation and decreases in GO treated samples in a dose dependent way. It appears that GO, in a concentration-related way and therefore depending on the surface available for cholesterol adsorption, favour extraction of cholesterol from the membrane thus confirming theoretical data that recently evidenced the capacity of graphene to extract cholesterol from membrane bilayer [22].

2.5. Effect of GO on spermatozoa adhesion

Sperm membranes are involved in interactions of spermatozoa with the surrounding environment and with the adhesion to different substrates. As it is evident in Fig. 7B, male gametes adhesion to substrates without or with GO, at different concentrations, change with the time, in a dose dependent manner.

Similarly, AFM experiments in Figs. 8 and 9 evidence the adhesion of the spermatozoa to the substrate during capacitation both in the absence and in the presence of GO, at different concentrations. In particular, in-phase images evidence, passing from T0 to T2, a change of the composition of the membrane in both control and GO-enriched samples, with a more homogeneous composition of the membrane at T0 and a more dishomogeneous composition at T2. Despite topography can affect also in-phase images and therefore data have to be treated with caution, these evidences confirm the change of composition of the membrane during capacitation in both the control and GO-enriched samples.

3. Discussion

Here we analysed the effect of GO on *in vitro* mammalian spermatozoa capacitation. The experimental model we used, swine spermatozoa, allow to reach this very important experimental goal adopting a protein free-system [23–25], in which it is possible to control the bioavailability of GO. In our opinion this is an extremely important methodological aspect, because it has been reported that GO could interact with albumin and other proteins [26], consequently up to now in the literature there is not an exact estimation of the real bioavailable GO. For this reason, as first, we identified the range of GO concentration able to promote biologically relevant effect, without being toxic. As it is evident from the data about sperm viability, the GO concentration exceeding 5 μg/mL are directly cytotoxic, therefore we decided to use the range between 5 μg/mL and 0.5 μg/mL. In this context, it is very interesting to note that the GO concentration of 5 μg/mL induced a statistically significant increase in the percentage of spermatozoa losing their acrosome integrity: this finding clearly indicates that GO is able to affect the functional status of spermatozoa plasma membrane thus potentially affecting their fertilizing ability.

Then we carried out an IVF experiment, comparing the effect of 0.5, 1 and 5 μg/mL GO. We found that, as expected, the concentration of 5 μg/mL have a detrimental effect on the percentage of fertilized oocytes, confirming a negative effect on male gametes fertilizing ability. Surprisingly, we found that 0.5 μg/mL and, more, 1 μg/mL display a positive effect on this parameter. Fertilization is a multistep process, in which sperm membranes play a key role. Indeed, they are composed by several regions (the domains): the apical ridge area, the pre-equatorial area, the equatorial area, the post-equatorial area, the midpiece and the tail. Each of them is characterized by a specific chemical composition and is involved in different biological activities (sperm egg interaction, exocytosis of acrosome content, motility, etc…). In turn, each domain contains specialized areas, the microdomains, organized in a liquid ordered phase (L_O) surrounded by a more fluid liquid disordered (L_D) area. They contain high concentrations of cholesterol, sphingomyelin, gangliosides, phospholipids with saturated long-acyl chains, and specific receptors and proteins such as glycosylphosphatidylinisotol (GPI) anchored proteins, caveolin and flotillin [24,27]. In addition, as it has been observed in others mammalian cells, the inner and the outer leaflet of membranes have a different chemical composition, with the aminophospholipids phosphatidylserine (PS) and phosphatidylethanolamine (PE) more concentrated in the inner leaflet and the choline phospholipids sphingomyelin (SM) and phosphatidylcholine (PC) more concentrated in the outer leaflet [28]. During capacitation, membranes undergo a deep rearrangement that affects their composition and their biophysical properties: several lipids displace from one leaflet to the other one, the membrane fluidity increases, and the activity of several enzymes is modulated,

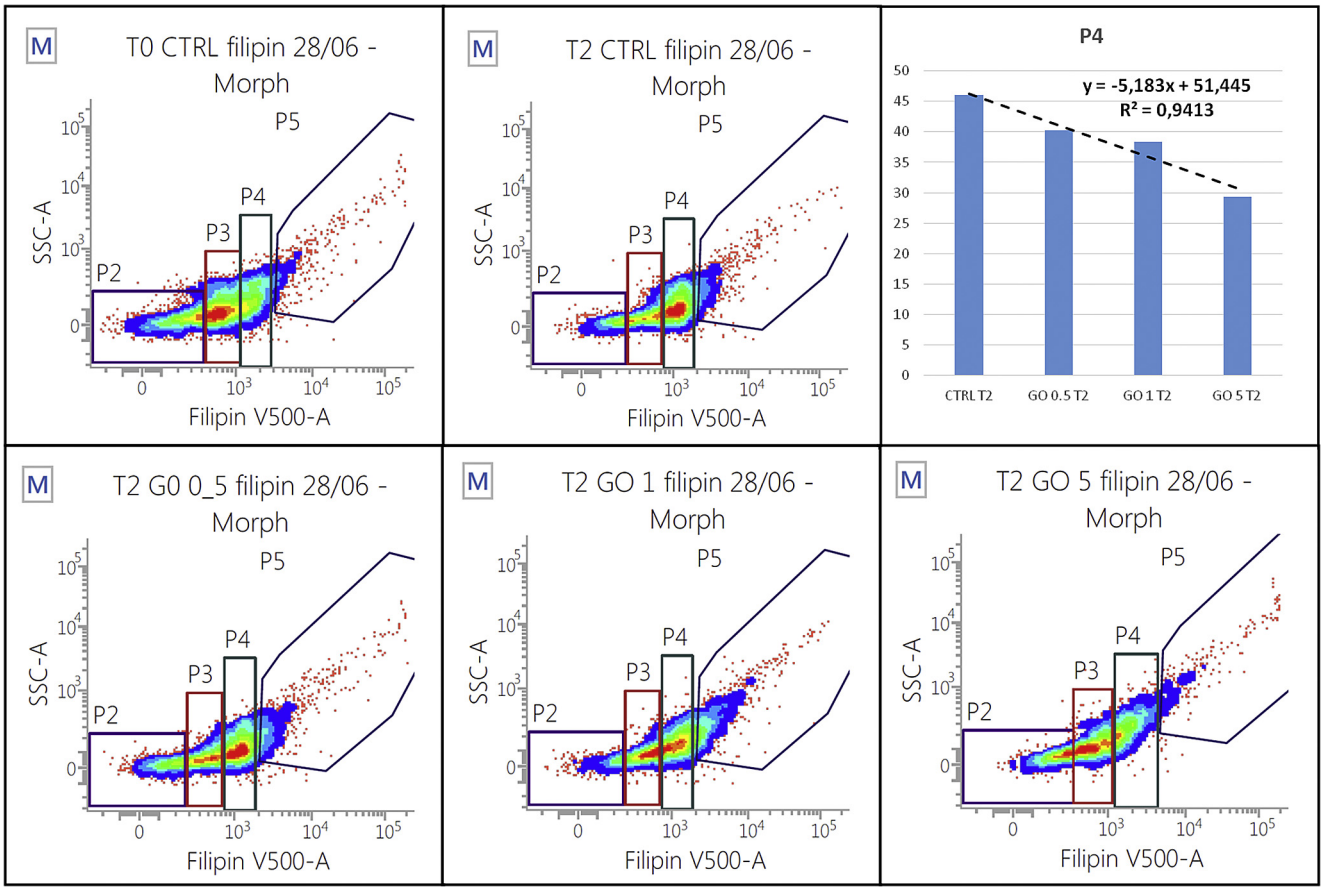

Fig. 6. Flow cytometry analysis of spermatozoa stained with filipin III and exposed to different GO concentrations. P2-P5 denote the different sperm subpopulation found in each sample, on the basis of filipin III emission and SSC value. The regression study (upper right panel) was carried out by calculating the Pearson's linear correlation coefficient (*r*). (A colour version of this figure can be viewed online.)

due to the activation of specific signalling pathways [29]. In particular, one of the key factors able to influence the functional behaviour of sperm membrane is the capacitation-dependent variations in cholesterol concentration and localization within membranes and, more in particular, in cholesterol/phospholipids ratio. All these changes involve specific subpopulations of cells, thus at any time different pools of cells are characterized by a different functional status. At the time of fertilization, the spermatozoa interact with the glycoproteins of oocyte zona pellucida and, successively, with the oocyte plasma membrane. The ability to recognize and bind them is the result of capacitation and directly determines the outcome of fertilization.

Then we can take two important inferences:

i) The sperm membrane is the site of interaction between GO and male gametes, as interface.
ii) The sperm membrane is the site of main signalling systems involved in the acquisition of fertilizing ability, which seems to be affected (either positively or negatively) by GO.

For these reasons, despite several papers [30–32] have recently reported that plausible mechanisms for GO interaction with cell membrane are either a GO aggregation that traps the cells or, more properly for bacteria, the rupture of the membrane by sharp edges, we have no evidence neither of GO aggregation nor of membrane rupture (see Fig. 9) and therefore we addressed our attention in assessing the possible effects exerted by GO on membrane physiology in our experimental model.

The results from FRAP analysis of CTRL samples are in perfect agreement with the predicted model: globally the CDC of DilC12 increases and new subpopulations characterized by higher values become detectable. It is noteworthy that the presence of GO in culture medium is able to induce significant changes on this parameter. Indeed, we found an effect on median values of CDC but especially marked differences in subpopulations present.

To best investigate this issue, we used the flow cytometry to identify possible variations in cholesterol trafficking due to the presence of GO. Physiologically, during capacitation, in experimental model in which extracellular proteins are present, cholesterol is removed from membranes by extracellular acceptor (albumin, serum proteins, etc.). On the contrary, in our model it is gradually exposed on outer leaflet of plasma membrane where it remains embedded. Actually, in CTRL condition we observe an increase of highly emitting subpopulation of spermatozoa (P4) from 22.9% at T0 to 46.0% after 2 h. In GO exposed samples we found a decrease in that population which highly correlates with the GO concentration ($r = -0.947$), thus suggesting that GO could be able to favour extraction of cholesterol from plasma membrane.

This result is in agreement with the theoretical data provided by Zhang and co-workers: the simulation they carried out shows that graphene is able of removing cholesterol from a bilayer membrane and that the hydrophilic portion of cholesterol molecules adsorbed onto the graphene sheet, prevents its internalization in the membrane bilayer [22]. In addition, the capacity of sodium deoxycholate, that is structurally very similar to cholesterol physiologically deriving from its oxidation, to adsorbe onto graphene favoring graphite

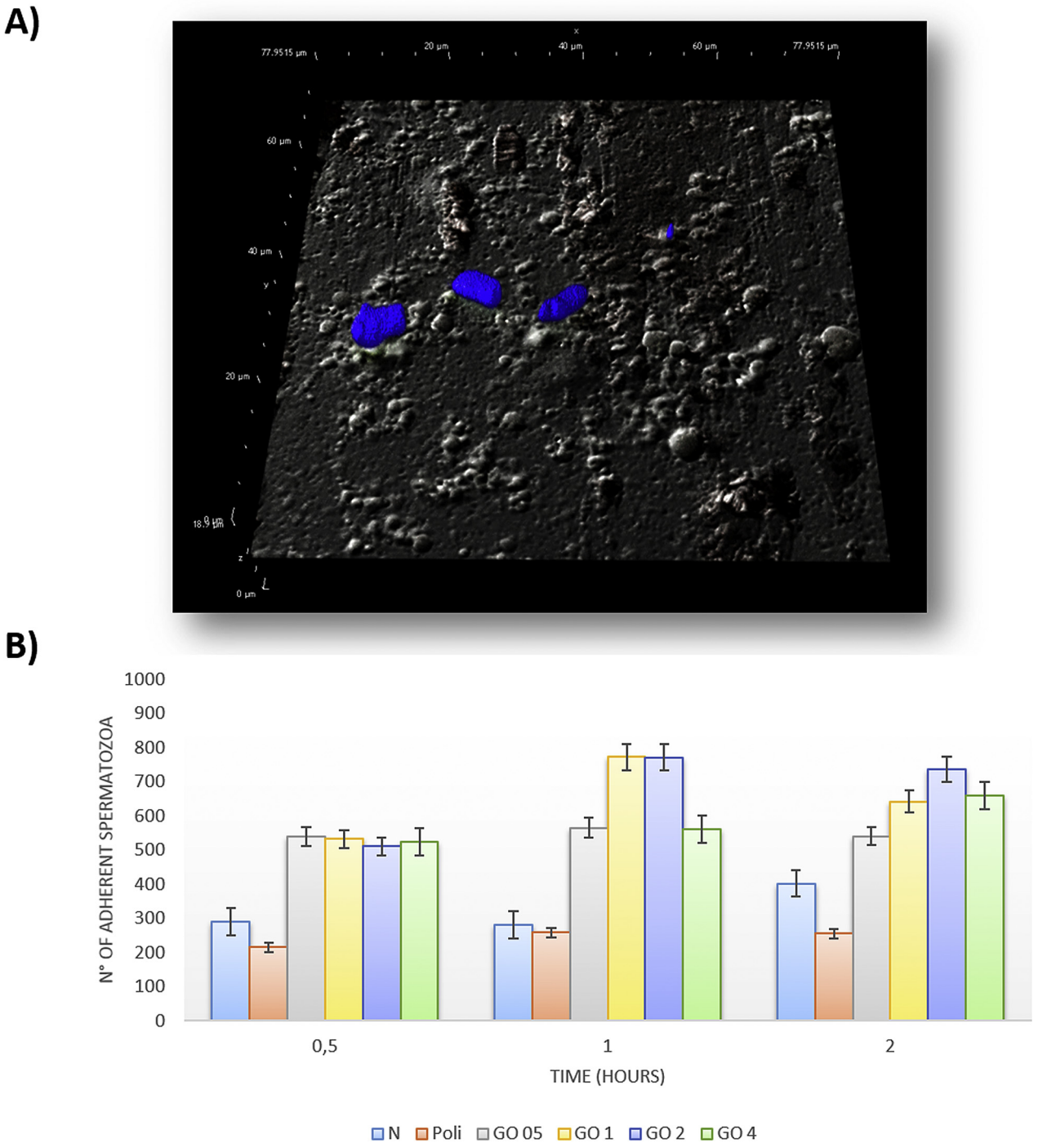

Fig. 7. A) confocal micrograph showing spermatozoa adherent to a GO coated slide (the spermatozoa nuclei are stained with DAPI). B) Results of spermatozoa adhesion experiment. Mean ± standard deviation were analysed with ANOVA two ways. Different superscripts indicate statistically different datasets. (A colour version of this figure can be viewed online.)

exfoliation [33] or to form a coating layer onto graphene oxide, has already been highlighted [34]. This means that sodium deoxycholate and consequently cholesterol have a high affinity for graphene oxide and it is plausible to speculate that, in proximity of graphene oxide, cholesterol tends to spread over the large graphene oxide surface.

Interestingly, the possible influence of GO exposure on membrane remodeling and on cholesterol extraction seems to be a specific characteristic of spermatozoa, indeed a recent evidence demonstrated that cholesterol did not vary in neurons treated with GO [35]. This could be due to the different biological mining of cholesterol and of cholesterol redistribution in biological membranes (i.e. in neurons also a cholesterol redistribution takes place) [36].

Still looking at membrane arrangement, we have found that the percentage of spermatozoa belonging to the subpopulation with the highest SSC and filipin values (P5), markedly changes after the cells incubation with GO. Interestingly, we found a very high correlation ($r = 0.969$) between the different relative amount of P5 and the IVF outcome at the different GO concentration. SSC value is proportional to cell granularity or complexity thus, once again, demonstrating the interaction of GO with sperm PM, probably

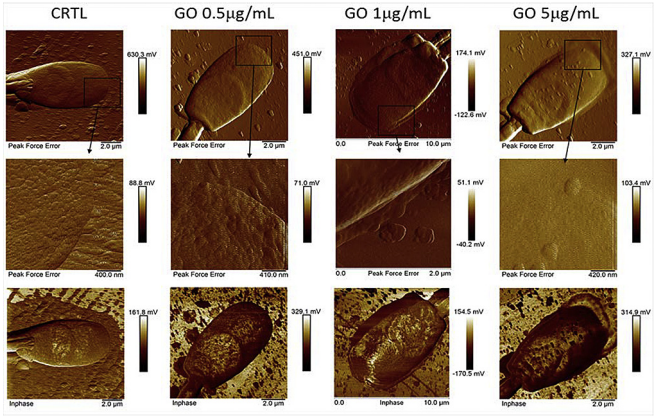

Fig. 8. AFM Peak Force error images of representative spermatozoa at T0 (images in the first row) in the control and in the presence of 0.5, 1 and 5 μg/mL GO. Images in the second row are insets from images of the corresponding first row. Images in the third row refer to corresponding AFM in-phase images. (A colour version of this figure can be viewed online.)

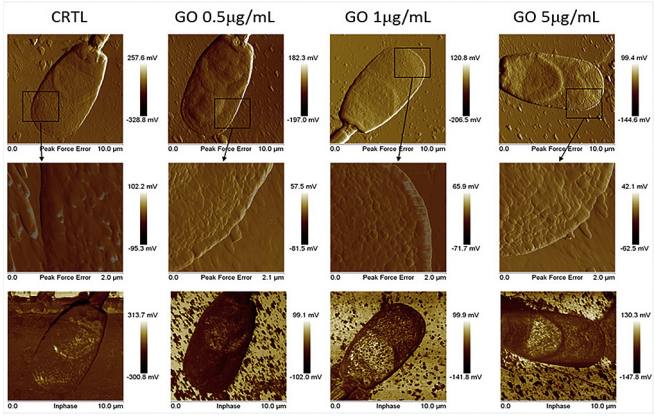

Fig. 9. AFM Peak Force error images of representative spermatozoa at T2 (images in the first row) in the control and in the presence of 0.5, 1 and 5 μg/mL GO. Images in the second row are insets from images of the corresponding first row. Images in the third row refer to corresponding AFM in-phase images. (A colour version of this figure can be viewed online.)

involving cholesterol, able to affect the process of fertilizing ability.

To confirm the GO effect on sperm membrane involving cholesterol trafficking and affecting cell adherence, we designed an appropriate experiment. As it is evident the number of spermatozoa adherent to the GO coated slides are significantly higher compared both with control samples and with poly-*l*-lysine coated slides. Moreover, from AFM micrographs (see Figs. 8 and 9), it appears evident that the spermatozoa membrane, in the presence GO, is integer thus confirming that GO does not enter in the cell but sensibly changes the membrane properties.

These membrane effects could affect per se the behavior of membrane and/or could induce alteration in membrane permeability, especially to ions, that could determine important effect on biochemical machinery involved in control of capacitation.

4. Conclusions

Here, we realized an experiment aimed to investigate the possible effects of GO exposure on male gametes. In our opinion they are an optimal model to study this issue, because they are virtually transcriptionally silent and their lipid metabolism is very limited [19,20], consequently they are unable to synthesize new molecules or to express new pathways in response to external stressors [37,38].

For the first time, we provide the evidence that GO could interfere with the acquisition of fertilizing ability of mammalian spermatozoa. Likely this effect is due to the interaction with membranes and, in particular, to the cholesterol extraction from plasma membrane. This datum could explain in one hand the toxicity of higher GO concentrations, in fact cholesterol is involved in maintaining plasma membrane stability, and in the other one hand could suggest possible new strategies to manage sperm capacitation.

5. Methods

5.1. Materials

GO was a commercial sample from Graphenea, San Sebastian, Spain. Elemental analysis evidenced 49–56% C, 0–1% H, 0–1% N, 2–4% S, 41–50% O and XPS spectrum the presence of C-C, C-O, C=O and O=C-O moieties, as extrapolated from product datasheet.

5.2. Spermatozoa preparation

After semen samples were collected and washed following an already standardized protocol [23,25] spermatozoa were incubated in the capacitation medium composed of TCM199 medium supplemented with 13.9 mM glucose, 1.25 mM sodium pyruvate, 2.25 mM calcium lactate and 100 μg/mL kanamycin (300 mOsm/kg, pH 7.4), at the final concentration of 0.5×10^7 cells/mL for at most 4 h at 38.5 °C in 5% CO_2 humidified atmosphere (Heraeus, Hera Cell). Only samples maintaining in control conditions (CTRL) a mean viability, assessed as previously described [38–40], of at least 90% at the end of the culture were considered for the following analysis. Different concentrations of GO (50, 10, 5, 1 and 0.5 μg/mL) were added to the medium containing spermatozoa, maintaining a control sample without GO. At T0 (just after adding cells to the incubation media), T1 (after 1 h of capacitation), T2, T3 and T4 different key aspects distinctive of the process of capacitation were evaluated.

5.3. Aqueous solution of graphene oxide

An aqueous solution of 4 mg/mL GO (GRAPHENEA, Donostia-San Sebastian, Spain) was diluted at the elected concentration, bath ultrasonicated for 10 min (Elmasonic P60H, 37 kHz, 180 W) and sterilized for 2 h under UV lamp (Spectronics Spectroline EF 160/C FE, 6 W, 50 Hz, 0.17 A). The concentration of GO was checked by UV–vis spectrophotometry at λ_{max} 230 nm. Dimensions of GO flakes were measured by using Dynamic Laser Light Scattering (90Plus/BI-MAS ZetaPlus multiangle particle size analyzer, Brookhaven Instruments Corp.) and AFM (Multimode 8, Bruker). Atomic force microscopy images were obtained operating in peak force QNM mode with ScanAsyst Air®, using a silicon cantilever and a RTESPA-300 tip (spring constant = 40 N/m, resonant frequency = 300 kHz). The specimen was prepared by spin-coating a 0.5 μg/mL GO dispersion onto silicon oxide wafer and placing the sample on the adhesive tape of the steel sample puck.

5.4. Monitoring of GO toxicity on acrosome integrity

Acrosome integrity was monitored by using a two staining technique with Hoechst 33258 and FITC-PSA able to identify alive unreacted and reacted spermatozoa [38,39]. At least 100 cells have been assessed by fluorescence microscopy in three independent experiments performed at different capacitation times (T0, T1, T2, T3 and T4), to the extent of CTRL or GO treated spermatozoa (50, 10, 5, 1 and 0.5 μg/mL GO).

5.5. Evaluation of GO toxicity on IVF experiments

To study the potential toxic effects of GO on spermatozoa fertilizing ability, an *in vitro* fertilization (IVF) assay was carried out using an already validated protocol [38]. Ovaries from pre-pubertal gilts were collected at a local slaughterhouse and transported to the laboratory within 1 h maintaining a temperature of 25 °C. After washing in a normal saline solution, ovaries were mechanically dissected under sterile conditions in Dulbecco's phosphate buffer with 0.4% BSA and 70 mg/L kanamycin. Isolated follicles from the ovaries of 4–5 mm diameter were selected on the basis of their translucent appearance, good vascularisation and compactness of their granulosa layer and cumulus mass. Healthy selected follicles were opened and oocytes were recovered. Maturation process to MII stage was obtained *in vitro* by culturing the follicles in Petri dishes containing 2 mL of TCM 199 medium added with 10% FCS, 70 mg/L kanamycin, ITS 10 mL/L and 1 mg/mL porcine LH and FSH and reversed inside out. The follicle walls were then placed on a stainless grid to avoid contact with the Petri dish bottom in this static system. After 44 h of culture oocytes were denuded in Hepes-TCM 199 with hyaluronidase on a warmed stage at 38.5 °C under a stereomicroscope. Only oocytes presenting the first polar body (MII stage) under the stereomicroscope were utilized for the IVF assay that was performed in fertilization medium [38]. Then *in vitro* capacitated spermatozoa, CTRL and treated with GO (5, 1, and 0.5 μg/mL) were added at the final concentration of 0.5×10^6 cells/mL. After 2 h the oocytes were gently removed from the Petri dish, transferred into fresh medium and maintained in culture for at least 12 h. The results of IVF have been expressed as fertilization rate (% of penetrated oocytes), incidence of polyspermy (% of polyspermic oocytes) and number of penetrating spermatozoa/polyspermic oocyte, according to already published researches [38,41].

We performed four independent experiment with a total number of 221 oocytes.

5.6. Evaluation of GO effect on spermatozoa membrane fluidity by fluorescence recovery after photobleaching (FRAP)

After washing, spermatozoa were cultured with capacitation medium (under control conditions or treated with GO 5, 1 and 0.5 μg/mL) containing the lipophilic fluorescent stain for labelling membranes DilC12(3) perchlorate (ultra pure) (ENZ-52206, Enzo Life Sciences, USA) used at the final concentration of 10 μM. Incubation was carried out during 15 min at 38.5 °C in 5% CO_2 humidified atmosphere (Heraeus, Hera Cell) with PBS and centrifuged for 10 min at 3000 rpm. FRAP experiments were performed at T0 and T2 capacitation times on the confocal microscope Nikon Ar1 laser confocal scanning microscope equipped with the NIS- Element software, using a Plan Apo λ 100X Oil objective (numerical aperture: 1.45; zoom: 1X; Refreactive Index: 1.515; pinhole size: 69 μm; 1 picture every 0.512 s). Fluorescence bleaching and recovery were conducted as follows: $\lambda_{exc} = 561.5$ nm; $\lambda_{em} = 595.5$ nm with 1 scan for basal fluorescence record at 2.4% of the maximum laser power, 1 scan at 100% laser power for bleaching, and 25 scans for monitoring recovery at 2.4% of the maximum laser power (see Fig. 2, upper panel). Recovery curves (average over at least 3 independent experiments for each group, i.e. performed on 7 different boar and in different days) were realized and analysed by using the simFRAP plug-in for Fiji ImageJ [42]. It computes the diffusion coefficients of the fluorescent dye embedded in cell membrane, regardless of bleaching geometry (Fig. 2, lower panel). The algorithm is based on fitting a computer-simulated recovery to actual recovery data of a FRAP series. In analysing our experiments, we set the requested parameters as following: pixel size: 0.12 μm; acquisition time per frame: 0.12 s. Results were expressed as diffusion coefficient (cm^2/sec).

5.7. Flow cytometry analysis of filipin III stain

To prove the depletion of cholesterol from the sperm membrane caused by GO the spermatozoa incubated in capacitation medium were stained at T0 and T2 with filipin III from *Streptomyces filipinensis* (Sigma-Aldrich), a polyene macrolide antibiotic used as a staining for free cholesterol. Previously cells were fixed with glutaraldehyde 4% during 30 min at 4 °C gently shaking and washed twice with PBS. The incubation with filipin III was carried out at a concentration of 25 μM for 30 min at room temperature gently shaking. Stained spermatozoa were observed with confocal microscopy or used for flow cytometry analysis.

To this second aim, 10.000 events/sample were acquired by flow cytometry (FACSVerse, BD Biosciences - three laser, eight color configuration, or FACSCanto, BD Biosciences - three laser, eight color configuration). Each reagent was titrated (8 point titration) under assay conditions; dilutions were established based on achieving the highest signal (mean fluorescence intensity, MFI) for the positive population and the lowest signal for the negative population, representing the optimal signal to noise ratio, and stain indexes were calculated. Instrument performances, data reproducibility and fluorescence calibrations were sustained and checked by the Cytometer Setup & Tracking Beads (BD Biosciences). In order to evaluate non-specific fluorescence, Fluorescence Minus One (FMO) controls were used. Compensation was assessed using CompBeads and FACSuite FC Beads (BD Biosciences) and single stained fluorescent samples. Data were analyzed using FACSuite v 1.0.5 (BD Biosciences) software.

5.8. Study of spermatozoa adherence to GO and atomic force microscopy

Spermatozoa adherence to GO was studied by using different types of slides in order to compare the adherence: control untreated slides, poly-L-lysine slides (ThermoFisher Scientific) and graphenated (0.5, 1, 2 and 4 mg/mL) slides. Graphenated slides were activated by UV Ozone-technique (PSD Series Digital UVO-zone System, Novascan) for 30 min 400 μL of 0.5, 1, 2 and 4 mg/mL GO aqueous solution were added of a small percentage of ethanol and spin coated (Laureil Model WS-650 Mz–23NPPB) sequentially at 500, 800 and 1600 rpm for 30 s onto the activated glass slides in order to obtain a homogeneous coating.

Similarly to the previous experiments, after collecting and washing, spermatozoa were cultured in capacitation medium. At T0 and T2 of capacitation, spermatozoa were transferred into the different slides for 5 min at 38.5 °C in 5% CO_2 humidified atmosphere. Slides were washed twice in a PBS solution with the purpose of removing non-adhered cells. The attached spermatozoa were automatically counted under confocal microscope (Fig. 7). The results showed the average of at least 9 field images from 3 different fields of each single slide. The experiment was performed twice, with 3 different boar samples.

Concurrently, spermatozoa adherence to GO was evaluated with the use of atomic force microscopy (AFM). Spermatozoa incubated under capacitated conditions (CTRL and treated with GO 5, 1, and 0.5 μg/mL) and at different times (T0, T1, T2, T3) were transferred into mini-slides (5 × 5 mm) rigorously washed with distilled H_2O and ethanol 90%. At least 3 samples of each time of capacitation and treatment were observed by AFM (Multimode 8, Bruker) to evaluate the attachment of spermatozoa to the slides, from three different boar models. Atomic force microscopy images were obtained operating in tapping mode in air, using a silicon cantilever and a RTESPA-150 tip (spring constant = 5 N/m, resonant frequency = 150 kHz). By using this mode it was possible to evaluate the topography as well as the phase, i.e. data connected with

surface stiffness/softness and chemistry of the surface, of the sample. The specimen was prepared by placing each sample on the adhesive tape of the steel sample puck.

5.9. Statistical analysis

The data were checked for normal distribution by D'Agostino and Pearson normality test, then they were compared by using parametrical or non-parametrical tests, following the needs. In the manuscript, the data are represented as mean ± standard deviation or as median [25° percentile-75° percentile] depending on their normalcy.

Author contributions

NB and AF conceived the experiments and wrote the manuscript; LV carried out the confocal microscopy experiments and realized the manuscript Figures; MRS participated in designing the experiments and in critically revising the manuscript; MRS, GC, and LG carried out the semen preparation and IFV experiments; PL, EE and MM carried out the flow cytometry experiments; RZ handled and characterized graphene oxide dispersions and performed AFM analyses. BB critically revised the manuscript. All authors have given approval to the final version of the manuscript.

Acknowledgment

MRS research was supported by MarieSkłodowska-Curie ITN REP-BIOTECH 675526, European Joint Doctorate in Biology and Technology of the Reproductive Health.

References

[1] K.S. Novoselov, A.K. Geim, S.V. Morozov, D. Jiang, Y. Zhang, S.V. Dubonos, et al., Electric field effect in atomically thin carbon films, Science 306 (2004) 666–669.
[2] A.K. Geim, Graphene : status and prospects, Science 324 (2009) 1530–1535.
[3] T. Kuilla, S. Bhadra, D. Yao, H. Hoon, S. Bose, H. Hee, Recent advances in graphene based polymer composites, Prog. Polym. Sci. 35 (2010) 1350–1375.
[4] S. Guo, S. Dong, Graphene nanosheet: synthesis, molecular engineering, thin film, hybrids, and energy and analytical applications, Chem. Soc. Rev. 40 (2011) 2644–2672.
[5] H.Y. Mao, S. Laurent, W. Chen, O. Akhavan, M. Imani, A.A. Ashkarran, et al., Graphene : promises, facts, opportunities, and challenges in nanomedicine, Chem. Rev. 113 (2013) 3407–3424.
[6] W. Guo, X. Zhang, X. Yu, S. Wang, J. Qiu, W. Tang, et al., Self-powered electrical stimulation for enhancing neural differentiation of mesenchymal stem cells on graphene–poly(3,4-ethylenedioxythiophene) hybrid microfibers, ACS Nano 10 (2016) 5086–5095.
[7] M. Radunovic, M. De Colli, P. De Marco, C. Di Nisio, A. Fontana, A. Piattelli, et al., Graphene oxide enrichment of collagen membranes improves DPSCs differentiation and controls inflammation occurrence, J. Biomed. Mater. Res. A 105 (2017) 2312–2320.
[8] A. Fabbro, D. Scaini, V. León, E. Vázquez, G. Cellot, G. Privitera, et al., Graphene-Based interfaces do not alter target nerve cells, ACS Nano 10 (2016) 615–623.
[9] Y. Kim, J. Lee, M.S. Yeom, J.W. Shin, H. Kim, Y. Cui, et al., Strengthening effect of single-atomic-layer graphene in metal–graphene nanolayered composites, Nat. Commun. 4 (2013) 3114/1–3114/7.
[10] V. Ettorre, P. De Marco, S. Zara, V. Perrotti, A. Scarano, Di Crescenzo, et al., *In vitro* and in vivo characterization of graphene oxide coated porcine bone granules, Carbon 103 (2016) 291–298.
[11] B. Zhang, P. Wei, Z. Zhou, T. Wei, Interactions of graphene with mammalian cells: molecular mechanisms and biomedical insights, Adv. Drug Deliv. Rev. 105 (2016) 145–162.
[12] Y. Zhang, S.F. Ali, E. Dervishi, Y. Xu, Z. Li, D. Casciano, et al., Cytotoxicity effects of graphene and single-wall carbon nanotubes in neural phaeochromocytoma-derived pc12 cells, ACS Nano 4 (2010) 3181–3186.
[13] Y.W. Chang, Sheng-Tao Yang, Jia-Hui Liu, H.W. Erya Dong, Aoneng Cao, Yuanfang Liu, *In vitro* toxicity evaluation of graphene oxide on A549 cells, Toxicol. Lett. 200 (2011) 201–210.
[14] B. Chaudhuri, D. Bhadra, L. Moroni, K. Pramanik, Myoblast differentiation of human mesenchymal stem cells on graphene oxide and electrospun graphene oxide–polymer composite fibrous meshes: importance of graphene oxide conductivity and dielectric constant on their biocompatibility, Biofabrication 7 (2015) 15009.
[15] D. Li, W. Zhang, X. Yu, Z. Wang, Z. Su, G. Wei, When biomolecules meet graphene : from and molecular level interactions to material design and applications, Nanoscale 8 (2016) 19491–19509.
[16] C. Bussy, H. Ali-Boucetta, K. Kostarelos, Safety considerations for graphene: lessons learnt from carbon nanotubes, Acc. Chem. Res. 46 (2013) 692–701.
[17] H. Yue, W. Wei, Z. Yue, B. Wang, N. Luo, Y. Gao, The role of the lateral dimension of graphene oxide in the regulation of cellular responses, Biomaterials 33 (2012) 4013–4021.
[18] J. Ma, R. Liu, X. Wang, Q. Liu, Y. Chen, R.P. Valle, Y.Y. Zuo, Crucial role of lateral size for graphene oxide in activating macrophages and stimulating pro-inflammatory responses in cells and animals, ACS Nano 9 (2015) 10498–10515.
[19] J.M. Vazquez, E.R.S. Roldan, Diacylglycerol species as messengers and substrates for phosphatidylcholine re-synthesis during Ca2+-dependent exocytosis in boar spermatozoa, Mol. Reprod. Dev. 48 (1997) 95–105.
[20] J.M. Vazquez, E.R.S. Roldan, Phospholipid metabolism in boar spermatozoa and role of diacylglycerol species in the de novo formation of phosphatidylcholine, Mol. Reprod. Dev. 47 (1997) 105–112.
[21] B. Barboni, N. Bernabò, P. Palestini, L. Botto, M.G. Pistilli, M. Chiarini, et al., Type-1 Cannabinoid receptors reduce membrane fluidity of capacitated boar sperm by impairing their activation by bicarbonate, PLos One 6 (2011), e23038.
[22] L. Zhang, B. Xu, X. Wang, Cholesterol extraction from cell membrane by graphene Nanosheets : a computational study, J. Chem. Phys. Chem. B 120 (2016) 957–964.
[23] M. Maccarrone, B. Barboni, A. Paradisi, N. Bernabò, V. Gasperi, M.G. Pistilli, Characterization of the endocannabinoid system in boar spermatozoa and implications for sperm capacitation and acrosome reaction, J. Cell Sci. 118 (2005) 4393–4404.
[24] N. Bernabò, M.G. Pistilli, M. Mattioli, B. Barboni, Role of TRPV1 channels in boar spermatozoa acquisition of fertilizing ability, Mol. Cell. Endocrinol. 323 (2010) 224–231.
[25] Q. Mu, G. Jiang, L. Chen, H. Zhou, D. Fourches, A. Tropsha, et al., Chemical basis of interactions between engineered nanoparticles and biological systems, Chem. Rev. 114 (2016) 7740–7781.
[26] T. Leahy, B.M. Gadella, New insights into the regulation of cholesterol efflux from the sperm membrane, Asian J. Androl. 17 (2000) 561–567.
[27] L. Botto, N. Bernabò, P. Palestini, B. Barboni, Bicarbonate induces membrane reorganization and CBR1 and TRPV1 endocannabinoid receptor migration in lipid microdomains in capacitating boar spermatozoa, J. Membr. Biol. 238 (2010) 33–41.
[28] B.M. Gadella, C. Luna, Cell biology and functional dynamics of the mammalian sperm surface, Theriogenology 81 (2014) 74–84.
[29] A. Romarowski, M.A. Battistone, F.A.,C. La Spina, C. Puga Molina del, G.M. Luque, A.L. Vitale, et al., PKA-dependent phosphorylation of LIMK1 and Cofilin is essential for mouse sperm acrosomal exocytosis, Dev. Biol. 405 (2015) 237–249.
[30] E. Hashemi, O. Akhavan, A. Shamsara, R. Rahighi, A. Esfandiard, A.R. Tayefeha, Cyto and genotoxicities of graphene oxide and reduced graphene oxide sheets on spermatozoa, RSC Adv. 4 (2014) 27213–27223.
[31] O. Akhavan, E. Ghaderi, A. Esfandiar, Wrapping bacteria by graphene nanosheets for isolation from environment, reactivation by sonication, and inactivation by near-infrared irradiation, J. Phys. Chem. B 115 (2011) 6279–6288.
[32] O. Akhavan, E. Ghaderi, Toxicity of graphene and graphene oxide nanowalls against bacteria, ACS Nano 4 (2010) 5731–5736.
[33] S. Wang, M. Yi, Z. Shen, The effect of surfactants and their concentration on the liquid exfoliation of graphene, RSC Adv. 6 (2016) 56705–56710.
[34] H.B. Park, H.W. Kim, Graphene oxide film coated with bile acid or bile salt, and manufacturing method therefor, PCT Int. Appl. (2016). WO 2016013796 A1 20160128.
[35] M. Bramini, S. Sacchetti, A. Armirotti, A. Rocchi, E. Vasquez, T. Bandiera, et al., Graphene oxide nanosheets disrupt lipid composition, Ca 2+ homeostasis, and synaptic transmission in primary cortical neurons, ACS Nano 10 (2016) 7154–7171.
[36] M. Aureli, S. Grassi, S. Prioni, S. Sonnino, A. Prinetti, Lipid membrane domanins in the brain, Biochim. Biophys. Acta 1851 (2015) 1006–1016.
[37] N. Bernabò, E. Tettamanti, M.G. Pistilli, D. Nardinocchi, P. Berardinelli, M. Mattioli, et al., Effects of 50 Hz extremely low frequency magnetic field on the morphology and function of boar spermatozoa capacitated *in vitro*, Theriogenology 67 (2007) 801–815, https://doi.org/10.1016/j.theriogenology.2006.10.014.
[38] N. Bernabò, E. Tettamanti, V. Russo, A. Martelli, M. Turriani, M. Mattoli, et al., Extremely low frequency electromagnetic field exposure affects fertilization outcome in swine animal model, Theriogenology 73 (2010) 1293–1305.
[39] N. Bernabò, P. Berardinelli, A. Mauro, V. Russo, P. Lucidi, M. Mattioli, et al., The role of actin in capacitation-related signaling: an in silico and *in vitro* study, BMC Syst. Biol. 5 (2011) 47.
[40] L.R. Abeydeera, B.N. Day, Fertilization and subsequent development *in vitro* of pig oocytes inseminated in a modified tris-buffered medium with frozen-thawed ejaculated spermatozoa, Biol. Reprod. 57 (1997) 729–734.
[41] https://imagej.nih.gov/ij/plugins/sim-frap/index.html.